Hong Kong J Radiol. 2022;25:84-93 | https://doi.org/10.12809/hkjr2217340

ORIGINAL ARTICLE **CME**

Utility of Liver Imaging Reporting and Data System v2018 Ancillary Features for the Diagnosis of Hepatocellular Carcinoma in LR-4 Lesions Using Contrast-enhanced Magnetic Resonance Imaging

K Lim, H Kwon, J Cho, D Kim, S Kim, E Kang

Department of Radiology, Dong-A University Hospital, Busan, Republic of Korea

ABSTRACT

Objective: *To evaluate the diagnostic performance of Liver Imaging Reporting and Data System (LI-RADS) version 2018 ancillary features for the diagnosis of hepatocellular carcinoma (HCC) from LR-4 ('probably HCC') lesions using gadoxetic acid–enhanced magnetic resonance imaging.*

Methods: *This retrospective study evaluated 166 LR-4 lesions including ancillary features in 114 high-risk cases imaged with gadoxetic acid–enhanced magnetic resonance imaging between March 2015 and December 2017. Two radiologists evaluated the imaging features using LI-RADS v2018. All lesions were confirmed as HCC or benign lesions by pathological assessment or >2 years of follow-up imaging. The diagnostic contribution of ancillary features was assessed using simple and multivariable logistic regression and generalised estimating equations.*

Results: *In all, 114 HCCs (68.7%) and 52 benign lesions (31.3%) were confirmed. Simple logistic regression analysis revealed that mild to moderate T2 hyperintensity ($p = 0.014$), restricted diffusion ($p < 0.001$), and intralesional fat ($p = 0.018$) were statistically significant for differentiating HCCs from benign lesions; however, multivariable logistic analysis revealed that only restricted diffusion was statistically significant (adjusted odds ratio = 9.703, $p < 0.001$). Restricted diffusion had lower sensitivity (48.2%) and higher specificity (90.4%) for the diagnosis of HCC; however, the diagnostic values improved when combined with mild to moderate T2 hyperintensity and hepatobiliary phase hypointensity (sensitivity: 73.8%, specificity: 80.8%).*

Conclusion: *Among ancillary LI-RADS v2018 imaging features, restricted diffusion is the diagnostic feature most accurately distinguishing HCCs from benign abnormalities in LR-4 lesions.*

Key Words: *Carcinoma, hepatocellular; Diagnostic imaging; Gadolinium ethoxybenzyl DTPA; Liver; Magnetic resonance imaging*

Correspondence: *Prof. H Kwon, Department of Radiology, Dong-A University Hospital, Busan, Republic of Korea*
Email: risual@dau.ac.kr

Submitted: 14 Feb 2021; Accepted: 13 May 2021

Contributors: HK designed the study. KL acquired the data. JC and SK analysed the data. DK drafted the manuscript. EK critically revised the manuscript for important intellectual content. All authors had full access to the data, contributed to the study, approved the final version for publication, and take responsibility for its accuracy and integrity.

Conflicts of Interest: All authors have disclosed no conflicts of interest.

Funding/Support: The study was supported by Dong-A University Research Fund.

Data Availability: All data generated or analysed during the present study are available from the corresponding author on reasonable request.

Ethics Approval: The study was approved by Dong-A Research Ethics Committee (Ref: DAUHIRB-20-087). The requirement for informed consent was waived because of the retrospective nature of the study. The patients were treated in accordance with the tenets of the Declaration of Helsinki. The patients provided written informed consent for all treatments and procedures.

中文摘要

肝臟成像報告和數據系統2018版輔助徵象對MRI從LR-4病變轉診為肝細胞癌的意義

K Lim、H Kwon、J Cho、D Kim、S Kim、E Kang

目的：評估肝臟成像報告和數據系統（LI-RADS）2018版輔助徵象對釓塞酸增強MRI從LR-4病變（“可能是 HCC”）轉診為肝細胞癌（HCC）的意義。

方法：本回顧研究分析2015年3月至2017年12月期間釓塞酸增強MRI 114例高危病例中的166個包含輔助徵象的LR-4病變。兩名放射科醫生使用LI-RADS 2018版評估成像特徵。所有病灶均通過病理或超過2年的隨訪影像學證實為HCC或良性病變。使用單變量和多變量邏輯迴歸和廣義估計方程評估輔助徵象對於診斷的貢獻。

結果：共確診114個HCC（68.7%）和52個良性病變（31.3%）。單變量邏輯迴歸分析顯示輕度至中度T2高信號（$p = 0.014$）、彌散受限（$p < 0.001$）和病灶內脂肪（$p = 0.018$）在區分HCC和良性病變具統計學意義；而多變量邏輯分析顯示，只有彌散受限具統計學意義（經調整比值比 = 9.703，$p < 0.001$）。彌散受限對HCC的診斷敏感性較低（48.2%），特異性較高（90.4%），然而當結合輕度至中度T2高信號和肝膽期低信號時，敏感性為73.8%，特異性為80.8%。

結論：在LI-RADS 2018版輔助影像學徵象中，彌散受限最能區分HCC與LR-4良性病變。

INTRODUCTION

Hepatocellular carcinoma (HCC) is the most common type of primary liver cancer in adults, and the most common cause of mortality in cirrhotic patients.[1] In 2011, the American College of Radiology introduced the Liver Imaging Reporting and Data System (LI-RADS) to standardise the acquisition, interpretation, and reporting of enhanced magnetic resonance imaging (MRI) or computed tomography imaging of liver lesions in patients at high risk of HCC. The most updated LI-RADS v2018 includes five major categories (LR-1 to LR-5) based on imaging features that reflect their relative probability of being benign or HCC.[2] The accuracy of the system for diagnosing HCC in the category ‘LR-4 (probably HCC)’ has been reported to be approximately 73% to 74%.[3,4] When LR-4 is reported, it is generally recognised as HCC requiring a pathological diagnosis or treatment, but the diagnostic accuracy of the LR-4 group is often a clinical dilemma to initiate immediate treatment without a pathological diagnosis.

When determining a LI-RADS v2018 category using MRI, five major features are considered: nonrim arterial phase hyperenhancement (APHE), nonperipheral washout, enhancing capsule, size, and threshold growth; ancillary features are additional imaging findings designed to improve detection accuracy and increase reliability. Ancillary features are not intended to be used without major features regardless of their abundance. They can be used optionally at the discretion of the radiologist when category adjustment is necessary, and only one category can be upgraded or downgraded. But any ancillary features cannot be used to upgrade to LR-5; upgrading an LR-4 to an LR-5 cannot currently be performed because there is not enough specificity for the diagnosis of HCC.[2] Thus, in the current LI-RADS, it can be said that LR-4 is made up of a rather heterogeneous group (ranging from upgrades from LR-3 to remained lesions that have not been upgraded to LR-5).

Since early diagnosis of HCC is important to increase the likelihood of treatment, it is important to increase the diagnostic accuracy of the LR-4 category. Several recent studies have reported the diagnostic performance of LI-RADS ancillary features.[5-7] However, the diagnostic performance of category adjustment and the

importance of each contributing ancillary feature have not been sufficiently studied, particularly in observations upgraded from LR-3 or downgraded from LR-4.

The goal of this study was to evaluate the diagnostic performance of LI-RADS v2018 ancillary features for improving the diagnostic accuracy for HCC in LR-4 lesions using gadoxetic acid–enhanced MRI. We also investigated whether using a certain combination of ancillary features could improve the diagnostic accuracy of the LR-4 category.

METHODS

Study Population

We retrospectively searched consecutive cases at high risk for HCC who underwent gadoxetic acid–enhanced MRI between March 2015 and December 2017. Inclusion criteria were as follows: (1) LR-3 and LR-4 lesions categorised on the basis of major imaging features, with one or more ancillary imaging features; (2) lesions confirmed as HCC or benign lesions through pathological diagnosis or subsequent imaging over 2 years. Exclusion criteria were as follows: (1) lesions difficult to characterise because of small size (<5 mm) or suboptimal image quality; (2) multifocal lesions (>5); (3) LR-M (probably or definitely malignant but not HCC specific) and LR-TIV (tumour in vein) lesions; and (4) administration of locoregional therapy before obtaining pathological proof without evidence of recurrence in subsequent imaging.

Liver Magnetic Resonance Imaging Protocols

The liver MRI was performed on a 3.0-Tesla system (Discovery MR750, GE Healthcare, Waukesha [WI], United States) with following protocols: localiser images using T2-weighted single-shot fast spin-echo sequence and chemical shift images using three-dimensional (3D) dual-echo T1-weighted gradient-echo sequence. Dynamic contrast-enhanced images were acquired with 15-s breath-hold interval before and after contrast agent injection using 3D-spoiled gradient-echo sequence with two-point Dixon water-fat separation (3D LAVA-FLEX). Contrast administration was performed at a dose of 0.1 mL/kg of gadoxetic acid at a rate of 1 mL/s followed by a 20-mL saline flush at the same rate. Dynamic contrast-enhanced images were obtained after contrast injection during the early arterial phase, late arterial phase, portal venous phase (PVP), transitional phase (TP), and hepatobiliary phase (HBP). T2-weighted image and diffusion-weighted image (DWI) were successively obtained using navigator triggering during the long interval between the TP and HBP. T2-weighted images were obtained using fat-saturated T2-weighted turbo spin-echo, known as PROPELLER (periodically rotated overlapping parallel lines with enhanced reconstruction) and DWIs were obtained at three b-values (50, 400, 800 s/mm^2). The apparent diffusion coefficient (ADC) images were generated automatically on the MR console system using a mono-exponential ADC model of all 3 b-values.

Lesion Registration

One radiologist (KL), with 6 years' experience with liver MRI, who was aware of patient clinical information, retrospectively reviewed the MRI exams and reports in a PACS (picture archiving and communication system), identifying consecutive observations fulfilling the inclusion criteria. When a target patient was identified, the reader recorded the size and location of individual lesions on the basis of major image features and selected the largest lesions up to a total of five if there were multiple lesions in one patient. After inclusion, two board-certified radiologists with >10 years of experience in MRI reviewed and verified the lesions.

Magnetic Resonance Imaging Analysis

Two other radiologists (HK and JC, with 16 years and 20 years of experience in liver MRI, respectively) performed image analysis according to the following steps. First, after lesion registration, two readers (HK and JC) blinded to the final lesion diagnosis assessed the presence or absence of all major and ancillary features individually within a week. Second, immediately after an individual assessment, all discordant major or ancillary features were discussed twice to achieve consensus in two separate sessions spaced apart by a week.

Reference Standards

All lesions included in the study were confirmed by pathological diagnosis or imaging follow-up. As defined in LI-RADS v2018, a lesion was considered benign in the following instances: (1) lesions that did not change in size or acquire additional imaging features >2 years of follow-up; (2) lesions that reduced in size or disappeared during imaging follow-up. Cases were considered HCC when: (1) lesions were pathologically confirmed by surgery or biopsy; (2) lesions increased in diameter ≥50% within 6 months (threshold growth) and lesion size >20 mm; (3) recurrent lesions after locoregional therapy (e.g., radiofrequency ablation, transarterial chemoembolisation). When a lesion suspected to be benign had ≤2 years of follow-up, it was excluded if

there was no size reduction or disappearance. Similarly, even if HCC was suspected, lesions with a stable size after locoregional therapy without pathological diagnosis were excluded.

Statistical Analysis

The potential association between ancillary imaging features and final diagnosis was evaluated using Pearson's Chi-square and binary logistic regression analysis. Simple and multivariable logistic regression analyses (using generalised estimation equations to avoid clustering effects) were performed to characterise potential associations between the presence of ancillary imaging features and HCC. Variables with $p \leq 0.20$ in the simple logistic regression analysis were then included in a multivariable logistic regression analysis. Multivariable logistic regression analysis was conducted with two models: Model 1 included significant variables among the ancillary imaging features and Model 2 included significant variables for all major and ancillary imaging features. Results were presented as the odds ratio (OR), 95% confidence interval (CI), p value, and considered statistically significant when $p \leq 0.05$. A binary diagnostic test was performed to estimate the diagnostic performance, and potential combinations of ancillary imaging features, which may contribute most to improving diagnostic performance, were also evaluated.

Statistical analyses were performed using SPSS (Windows version 23.0; IBM Corp., Armonk [NY], United States).

RESULTS

The final sample consisted of 114 cases (88 male and 26 female), with a mean age of 65.5 ± 9.4 years (range, 37-87) [Table 1].

Lesion Characteristics

A total of 166 lesions were included in the study, with a mean lesion diameter of 12.3 ± 5.4 mm and a mean of 1.4 ± 0.8 (range, 1-5) lesions per patient (1 lesion, n = 90; 2 lesions, n = 21; 3 lesions, n = 10; 4 lesions, n = 1). Category adjustments were performed according to the LI-RADS algorithm, on the basis of ancillary features in all lesions, as follows: 133 LR-3 lesions were upgraded to LR-4, 4 LR-4 were not adjusted because they had ancillary features that favoured both malignancy and benignity, and 29 LR-4 lesions were not upgraded to LR-5 even though they had ancillary features favouring HCC or malignancy. These were confirmed as 114 HCCs (68.7%) and 52 benign lesions (31.3%) [Figure 1].

Table 1. Characteristics of study populations.*

Variables	Male (n = 88)	Female (n = 26)	Total (n = 114)
Age, y			
Mean ± SD	64.7 ± 9.2	68.1 ± 9.6	65.5 ± 9.4
Range	37-82	49-87	37-87
Aetiology of cirrhosis			
HBV	32 (36.4%)	10 (38.5%)	42 (36.8%)
HCV	14 (15.9%)	9 (34.6%)	23 (20.2%)
Alcohol	18 (20.5%)	2 (7.7%)	20 (17.5%)
HBV + HCV	2 (2.3%)	1 (3.8%)	3 (2.6%)
Alcohol + HBV	12 (13.6%)	-	12 (10.5%)
Alcohol + HCV	7 (8.0%)	1 (3.8%)	8 (7.0%)
Alcohol + HBV + HCV	1 (1.1%)	-	1 (0.9%)
Autoimmune hepatitis	-	1 (3.8%)	1 (0.9%)
Polycythaemia vera	1 (1.1%)	-	1 (0.9%)
Cryptogenic	1 (1.1%)	2 (7.7%)	3 (2.6%)

Abbreviations: HBV = hepatitis B virus; HCV = hepatitis C virus; SD = standard deviations.
* Data are shown as No. (%), unless otherwise specified.

Diagnostic Performance of the Imaging Features

Lesions were divided by size: <10 mm, 10 to 19 mm, and ≥20 mm.

Among all evaluated ancillary features, HBP hypointensity was most common (150 of 166) and had the highest sensitivity (92.1%) with lowest specificity (13.5%). Mild to moderate T2 hyperintensity was relatively common (108 of 166) and had relatively high sensitivity (71.2%) with low specificity (46.2%). Restricted diffusion was relatively less common (60 of 166) and had high specificity (90.4%) with high positive predictive value (91.7%) [Table 2].

A nonenhancing capsule (10 of 166), intralesional fat (24 of 166), and HBP isointensity (16 of 166) were less common; however, a nonenhancing capsule appeared relatively more frequently in HCC compared with intralesional fat and HBP isointensity. Corona enhancement, fat sparing in a mass, nodule-in-nodule architecture, mosaic architecture, and marked T2 hyperintensity were rarely observed (≤5). We also analysed the major features of the included lesions and noted that nonrim APHE was the most common major feature (100 of 166) with a sensitivity of 68.4%. Nonperipheral washout in the PVP was relatively common (75 of 166), but the diagnostic performance was equivocal. Enhancing capsule was rarely observed (12 of 166) but showed the highest specificity (98.1%) and high positive predictive value (91.7%) [Table 2].

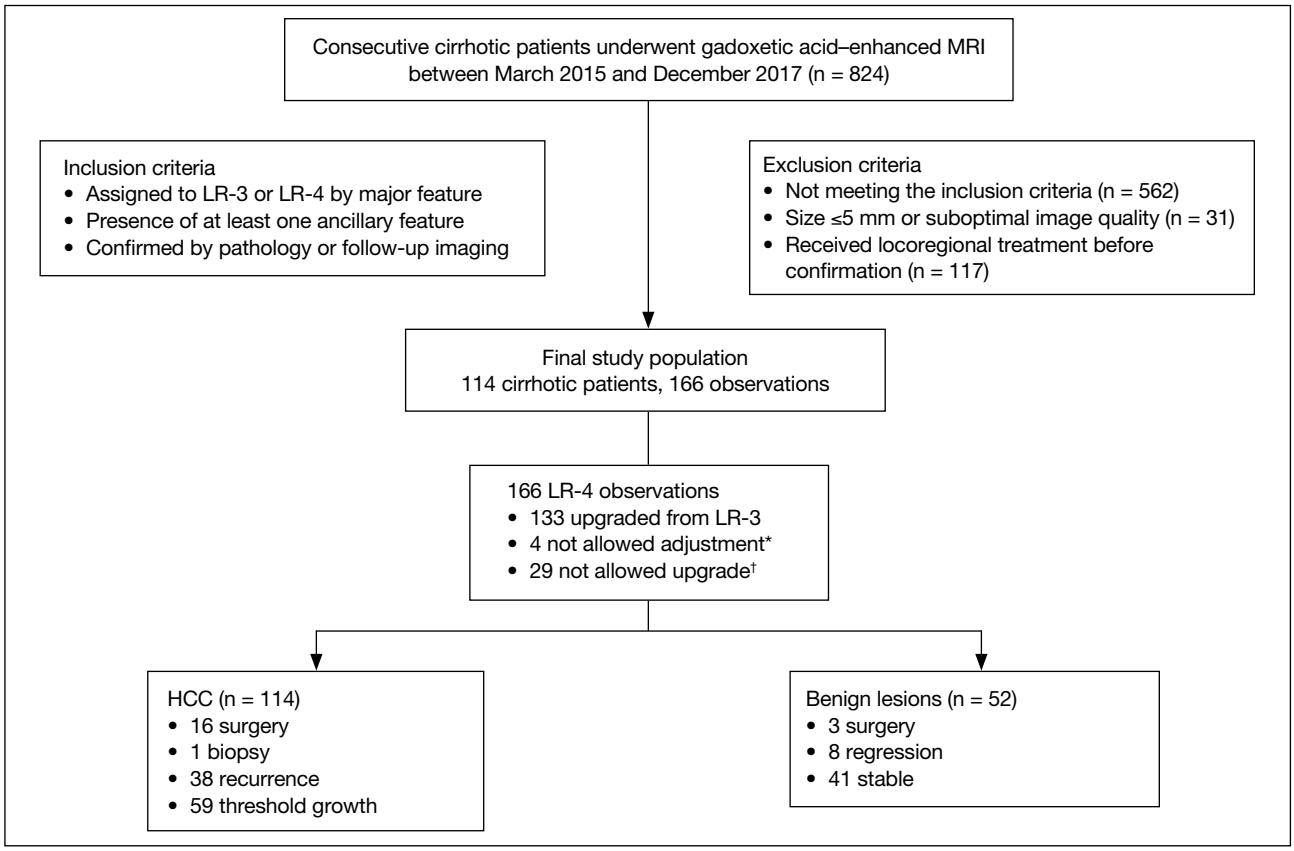

Figure 1. Study population flowchart.
Abbreviations: HCC = hepatocellular carcinoma; MRI = magnetic resonance imaging.
* Category adjustment not allowed because the lesion demonstrated ancillary features favouring benignity and HCC (or malignancy).
† Upgrading to LR-5 not allowed even if lesion demonstrated ancillary features favouring HCC or malignancy.

Table 2. Diagnostic performance of imaging features for distinguishing 114 hepatocellular carcinomas from 52 benign nodules.

Imaging features	No. of lesions				Sensitivity (%)	Specificity (%)	Accuracy (%)	PPV (%)	NPV (%)
	TP	FN	FP	TN					
Ancillary features									
Mild to moderate T2 hyperintensity	81	33	27	24	71.2	46.2	65.1	75	40
Restricted diffusion	55	59	5	47	48.2	90.4	68.7	91.7	44.3
Transitional phase hypointensity	81	33	38	14	71.1	27	71.7	71.1	29.8
Hepatobiliary phase hypointensity	105	9	45	7	92.1	13.5	67.5	70	43.8
Corona enhancement	1	113	0	52	0.9	100	31.9	100	31.5
Fat sparing in mass	1	113	0	52	0.9	100	31.9	100	31.5
Nonenhancing capsule	8	106	2	50	7	96.2	34.9	80	32.1
Nodule-in-nodule architecture	3	111	1	51	2.6	98.1	32.5	75	31.5
Mosaic architecture	4	110	0	52	3.5	100	33.7	100	32.1
Intralesional fat	12	102	12	40	10.5	76.9	31.3	50	28.2
Marked T2 hyperintensity	1	113	0	52	0.9	100	31.9	100	31.5
Hepatobiliary phase isointensity	8	106	8	44	7	84.6	31.3	50	29.3
Major features									
Size <10 mm	39	75	23	29	34.2	55.8	41	62.9	17.9
Size 10-19 mm	65	49	23	29	57	55.8	56.6	73.9	37.2
Size ≥20 mm	10	104	5	47	8.8	90.4	34.3	66.7	31.1
Nonrim APHE	78	36	22	30	68.4	57.7	65.1	78	45.5
Nonperipheral washout	44	70	31	21	38.6	40.4	39.2	58.7	23.1
Enhancing capsule	11	103	1	51	9.6	98.1	32.7	91.7	33.1

Abbreviations: APHE = arterial phase hyperenhancement; FN = false negative; FP = false positive; NPV = negative predictive value; PPV = positive predictive value; T2 = T2-weighted image; TN = true negative; TP = true positive.

Simple and Multivariable Logistic Regression Analyses

Simple logistic regression analysis revealed that among ancillary features — mild to moderate T2 hyperintensity ($p = 0.014$), restricted diffusion ($p < 0.001$), intralesional fat ($p = 0.018$), and among major features — nonrim APHE ($p = 0.001$) and nonperipheral washout ($p = 0.009$), were significantly associated with HCC. Other less common ancillary features were not included in the subsequent analyses. Multivariable logistic regression analysis with Model 1 revealed that only restricted diffusion was a significant and independent predictor of HCC (adjusted OR = 9.07, 95% CI = 2.89-28.53; $p < 0.001$) [Table 3]. Results from Model 2 demonstrated that restricted diffusion (adjusted OR = 7.42, 95% CI = 2.27-24.27; $p = 0.001$) and enhancing capsule (adjusted OR = 9.13, 95% CI = 1.72-48.35; $p = 0.009$) were significant (Table 3).

DISCUSSION

Advances in liver MRI technology (e.g., DWI, dynamic imaging, HBP imaging using hepatocyte-specific contrast agents) have enabled MR imaging to accurately assess tumour cellularity, vascularity, and absence of functioning hepatocytes.[8,9] These MR sequences can help facilitate early diagnosis of small HCCs through more detailed and accurate image analysis, rather than applying a wait-and-see policy, especially for suspected lesions at this stage (Figure 2). According to LI-RADS v2018, a lesion can be considered LR-4 if APHE is present along with at least one of three major features (i.e., nonperipheral washout, enhancing capsule, threshold growth), and, even if APHE is absent, the presence of two or more of three major features in a lesion can allow it to be considered as LR-4.[10] The most recent 2018 American Association for the Study of Liver Diseases practice guidelines[11,12] propose to apply stringent imaging criteria with high specificity for noninvasive diagnosis of HCC in high-risk patients. Key imaging features include size ≥1 cm, APHE, and combination with washout appearance and/or enhancing capsule. In addition, they emphasise a multidisciplinary diagnostic approach, particularly for LR-4 lesions measuring ≥1 cm in diameter. The LR-4 lesions are considered probable HCC, but sometimes subsequent image follow-ups are proposed without immediate action due to high false-positive rates (up to 30%). However, up to 15% of these untreated LR-3 lesions and 68% of untreated LR-4 lesions eventually become LR-5 within 2 years of follow-up.[11]

LI-RADS ancillary features are an option for radiologists and their use is encouraged because they exhibit various contrast enhancement patterns reflecting the histological characteristics of the tumour, even though they lack the specificity for accurate HCC diagnosis of

Table 3. Results of simple and multivariable logistic regression analyses of imaging features.*

Imaging features	Univariate analysis		Multivariate analysis (Model 1†)		Multivariate analysis (Model 2‡)	
	Unadjusted OR	p Value	Adjusted OR	p Value	Adjusted OR	p Value
Ancillary features						
Mild to moderate T2 hyperintensity	2.35 (1.19-4.65)	0.014	0.85 (0.37-3.40)	0.691	0.86 (0.33-2.23)	0.759
Restricted diffusion	9.75 (3.46-27.50)	<0.001	9.07 (2.89-28.53)	<0.001	7.42 (2.27-24.27)	0.001
Transitional phase hypointensity	0.93 (0.46-1.87)	0.838	-	-	-	-
Hepatobiliary phase hypointensity	2.25 (0.84-5.93)	0.101	1.26 (0.46-3.41)	0.655	2.45 (0.82-7.30)	0.109
Nonenhancing capsule	2.89 (0.48-17.56)	0.247	-	-	-	-
Nodule-in-nodule architecture	1.31 (0.18-9.85)	0.790	-	-	-	-
Intralesional fat	0.34 (0.14-0.83)	0.018	0.41 (0.16-1.02)	0.055	0.57 (0.21-1.56)	0.276
Hepatobiliary phase isointensity	0.44 (0.17-1.17)	0.101	0.79 (0.29, 2.17)	0.655	0.41 (0.14-1.22)	0.109
Major features						
Size <10 mm	0.58 (0.30-1.14)	0.116	-	-	0.10 (0.01-2.41)	0.156
Size 10-19 mm	1.67 (0.85-3.30)	0.137	-	-	1.20 (0.38-3.83)	0.759
Size ≥20 mm	0.99 (0.36-2.73)	0.980	-	-	-	-
Nonrim APHE	2.98 (1.55-5.73)	0.001	-	-	11.43 (0.67-194.13)	0.092
Nonperipheral washout	0.42 (0.22-0.80)	0.009	-	-	2.75 (0.18-41.75)	0.466
Enhancing capsule	6.44 (0.65-63.72)	0.111	-	-	9.13 (1.72-48.35)	0.009

Abbreviations: APHE = arterial phase hyperenhancement; OR = odds ratio; T2 = T2-weighted.

* Data are shown as adjusted or unadjusted OR (95% confidence interval), unless otherwise specified.

† Included only variables with p values <0.20 in the simple logistic regression analysis among the ancillary imaging features.

‡ Included only variables with p values <0.20 in the simple logistic regression analysis for all major and ancillary imaging features.

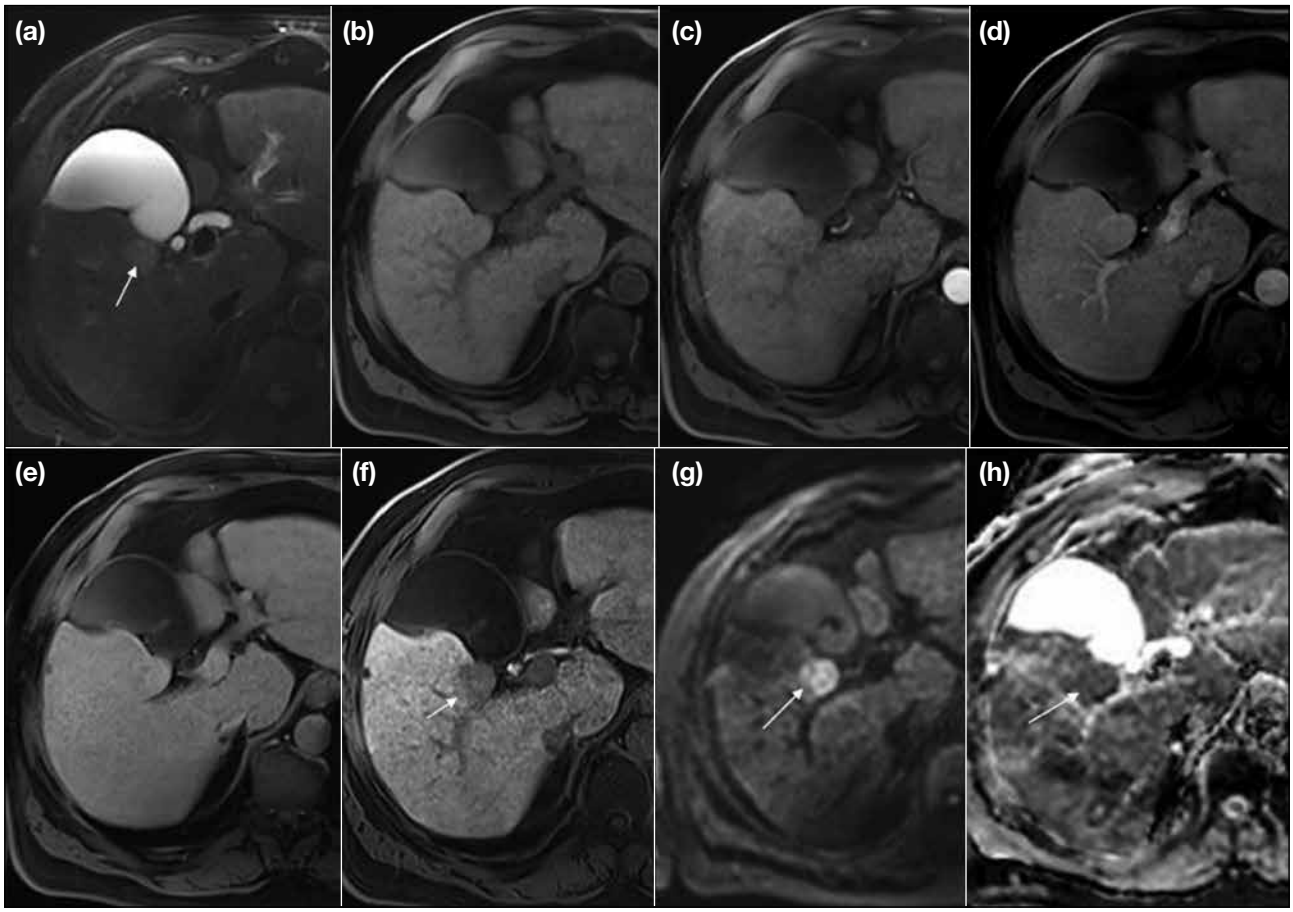

Figure 2. A 66-year-old man with hepatitis B–related liver cirrhosis. (a) Axial T2-weighted image showing a 17 mm mild-to-moderate hyperintensity lesion in segment V. (b) The precontrast axial T1-weighted image showing slightly hypointensity. Gadoxetic acid–enhanced (c) arterial, (d) portal, (e) transitional, and (f) hepatobiliary phase images showing no enhancement and no washout appearance with hepatobiliary hypointensity. (g) Diffusion-weighted image (b-value of 800 s/mm^2) and (h) apparent diffusion coefficient image showing restricted diffusion. The final Liver Imaging Reporting and Data System (LI-RADS v2018) category was LR-4. A surgical specimen was obtained 1 week after this examination, and the final pathological diagnosis was hepatocellular carcinoma.

major features. Recent studies characterising the clinical application of ancillary features[13-17] have shown that 15% to 35% of lesions were readjusted to a different LI-RADS category, with slightly more frequent upgrades than downgrades; in fact, roughly 63% of LR-4 lesions were upgrades from LR-3. We already know that major imaging features have high specificity for the diagnosis of HCC in LI-RADs lesions including LR-4. However, in clinical practice, a large percentage of LR-4 lesions are category upgraded to LR-4 from LR-3 lesions. Hence, improving diagnostic value among the ancillary features is important to increase specificity for the diagnosis of HCC of the LR-4 group. We believe that there is a difference in importance among the various ancillary features suggesting HCC.

Several studies have reported that mild to moderate T2 hyperintensity, TP hypointensity, and HBP hypointensity increase sensitivity for the diagnosis of HCC when used in combination with major features.[13,18-20]

Vernuccio et al[21] reported that the finding of HBP hypointensity significantly improves sensitivity for HCC diagnosis in LR-3 lesions measuring 10 to 19 mm with APHE while maintaining moderately high specificity. Kwon et al[22] reported that hyperintensity on T2-weighted images, in addition to arterial enhancement on gadoxetic acid–enhanced MR images, and hyperintensity on DWI, is helpful for differentiating small HCCs (≤2 cm) from benign nodules in patients with cirrhosis. Our data showed that HBP hypointensity (92.1%) has the highest sensitivity among major imaging features, and mild to moderate T2 hyperintensity (71.2%), TP hypointensity (71.1%) have relatively high sensitivity. However,

multivariable logistic regression analysis demonstrated that none of these values were statistically significant.

Restricted diffusion (90.4%), nonenhancing capsule (96.2%), intralesional fat (76.9%), and HBP isointensity (84.6%) showed a high specificity among relatively commonly appearing ancillary features. Uncommon ancillary features were considered to have high specificity, but their infrequency limits their utility for estimating diagnostic performance. Multivariable logistic regression analysis revealed that restricted diffusion was the only statistically significant for diagnosing HCC in both Model 1 (adjusted OR = 9.07; $p < 0.001$) and Model 2 (adjusted OR = 7.42; $p = 0.001$). Several studies have investigated the role of DWI to differentiate between HCCs and dysplastic nodules.[13,21,23-28] Granata et al[23] and Lee et al[24] reported a sensitivity of 81% to 84%, and specificity of 73% to 100% for 'hyperintensity on DWI'. Piana et al[25] reported that 'APHE combined with DWI hyperintensity' improves sensitivity for the diagnosis of HCC compared to conventional criteria, from 60% to 76%-77% for all HCCs, and from 37% to 60%-66% for HCCs <2 cm. In this study, restricted diffusion demonstrated a sensitivity of 48.2% and a specificity of 90.4% with statistical significance, which is similar to the sensitivity of 54.8% and specificity of 90.6% reported by Cerny et al.[13] Interestingly, although there were some differences in the study populations, these two studies showed lower sensitivity and higher specificity compared to other published studies as a result of strict application of the definition of restricted diffusion (i.e., hyperintensity on DWI and hypointensity on ADC images). In LI-RADS v2018, restricted diffusion is classified as an ancillary feature favouring malignancy in general (but not specific in HCC) and is defined as 'intensity on DWI unequivocally higher than liver and/or ADC unequivocally lower than liver'. Restricted diffusion is generally known to be useful in differentiating a malignant from a benign lesion, and is defined as having higher signal intensity, not attributable solely to T2 shine-through effect on DWI acquired with at least moderate diffusion weighting (e.g., b-value ≥400 s/mm^2). However, it was noted here that there were a very large number of false-positives when features were defined as 'hyperintensity on DWI or hypointensity on ADC image'. Therefore, a consensus was formed by strictly applying the definition of restricted diffusion as 'hyperintensity on DWI and hypointensity on ADC images', and the results showed a significant correlation with HCC. Although many studies about the diagnostic performance of DWI for the diagnosis of HCC have been reported based on 'hyperintensity on DWI',[22-24] the results presented here demonstrate that applying a strict definition reduces sensitivity, improves specificity, and maintains accuracy. Therefore, this study demonstrates that restricted diffusion may play a useful role in ancillary features for LR-4 lesions. Further research using a larger population is warranted, and it may be necessary to correct and supplement the definition of restricted diffusion mentioned in LI-RADS v2018.

In our study, the overall diagnostic performance of major features was lower compared with previous analyses.[13,21,22] APHE demonstrated intermediate diagnostic performance, nonperipheral washout had both low sensitivity and specificity, and enhancing capsule demonstrated very high specificity. The diagnostic performance of major imaging features in our study is thought to be somewhat lower than that of other studies on LR-4, since it was calculated on LR-4 that did not restrict a specific major features (e.g., size or APHE). Our data revealed that 33 cases of HCC showing only nonperipheral washout and/or capsular appearance without APHE. Therefore, it is considered that there may be selection bias when limiting studies of category up to LR-4.

Low diagnostic performance of nonperipheral washout for the diagnosis of HCC was reported here, a finding that may be related to characteristics of gadoxetic acid–enhanced imaging evaluation during the PVP only. It can be a variable in clinical practice, considering that the likelihood of nonperipheral washout being false-negative will be higher than expected, if problems occur in the process of enhancement or PVP cannot be accurately obtained.

An assessment of diagnostic criteria revealed that the specificity for the diagnosis of HCC when APHE was combined with nonperipheral washout or capsular appearance was 92%, consistent with previous studies showing specificity between 89% and 99%.[11,12,29]

The combination of major and ancillary features calculated in our study (e.g., APHE with DWI and APHE with HBP) did not reveal an improvement of diagnostic performance, unlike previous studies by Cerny et al[13] and Kwon et al.[22] Our calculated diagnostic value when combining major and ancillary features was similar to that calculated for each ancillary feature alone. The diagnostic performance of restricted diffusion, which showed the only statistical correlation with HCC

in multivariable logistic regression analysis, was best improved to 73.8% for sensitivity, 80.8% for specificity, and 75.5% for accuracy when combined with mild to moderate T2 hyperintensity and HBP hypointensity. These results show the role of ancillary features for diagnosis of HCC in LR-4 lesions. Additional studies are warranted to better understand comprehensive diagnostic criteria including ancillary imaging features.

There were several important limitations of this study. First, the study was performed retrospectively at a single institution, and there may have been selection bias of the study population. Second, confirmation of many lesions was made by subsequent imaging. Only 13.9% (23 of 166) of lesions included pathological diagnoses, however, there is an inevitable limitation because subsequent imaging is generally favoured at this stage, rather than pathological diagnosis. However, the reference standard was strictly applied and only cases with obvious features in subsequent imaging were included in this study population. Third, the final diagnosis was divided into HCC and benign lesions. Although confirmation through subsequent imaging was based, it was possible that unconfirmed non-HCC lesions were included in the HCC category; this effect was unpredictable.

In conclusion, our study to evaluate the diagnostic performance of ancillary features for the diagnosis of HCC in an LR-4 lesion suggest that restricted diffusion is the most useful diagnostic feature and is associated with excellent specificity. In case of LR-4 lesions with ancillary features, the combination of mild to moderate hyperintensity on T2 image and DWI restriction can improve the diagnostic value.

REFERENCES

1. World Health Organization. Cancer Today. 2018. Available from: https://gco.iarc.fr/today/online-analysis-table?v=2018&mode=cancer&mode_population=continents&population=900&populations=900&key=asr&sex=0&cancer=39&type=1&statistic=5&prevalence=0&population_group=0&ages_group%5B%5D=0&ages_group%5B%5D=17&group_cancer=1&include_nmsc=1&include_nmsc_other=1. Accessed 21 Sep 2019.
2. American College of Radiology. Liver Imaging Reporting and Data System version 2018. 2018. Available from: https://www.acr.org/-/media/ACR/Files/RADS/LI-RADS/LI-RADS-2018-Core.pdf?la=en. Accessed 21 Sep 2019.
3. Ronot M, Fouque O, Esvan M, Lebigot J, Aubé C, Vilgrain V. Comparison of the accuracy of AASLD and LI-RADS criteria for the non-invasive diagnosis of HCC smaller than 3 cm. J Hepatol. 2018;68:715-23.
4. van der Pol CB, Lim CS, Sirlin CB, McGrath TA, Salameh JP, Bashir MR, et al. Accuracy of the liver imaging reporting and data system in computed tomography and magnetic resonance image analysis of hepatocellular carcinoma or overall malignancy — a systematic review. Gastroenterology. 2019;156:976-86.
5. Cannella R, Vernuccio F, Sagreiya H, Choudhury KR, Iranpour N, Marin D, et al. Liver Imaging Reporting and Data System (LI-RADS) v2018: diagnostic value of ancillary features favoring malignancy in hypervascular observations ≥10 mm at intermediate (LR-3) and high probability (LR-4) for hepatocellular carcinoma. Eur Radiol. 2020;30:3770-81.
6. Cerny M, Chernyak V, Olivié D, Billiard JS, Murphy-Lavallée J, Kielar AZ, et al. LI-RADS version 2018 ancillary features at MRI. Radiographics. 2018;38:1973-2001.
7. Kang JH, Choi SH, Byun JH, Kim DH, Lee SJ, Kim SY, et al. Ancillary features in the Liver Imaging Reporting and Data System: how to improve diagnosis of hepatocellular carcinoma ≤3 cm on magnetic resonance imaging. Eur Radiol. 2020;30:2881-9.
8. Seale MK, Catalano OA, Saini S, Hahn PF, Sahani DV. Hepatobiliary-specific MR contrast agents: role in imaging the liver and biliary tree. Radiographics. 2009;29:1725-48.
9. Taouli B, Koh DM. Diffusion-weighted MR imaging of the liver. Radiology. 2010;254:47-66.
10. Rimola J, Forner A, Tremosini S, Reig M, Vilana R, Bianchi L, et al. Non-invasive diagnosis of hepatocellular carcinoma ≤2 cm in cirrhosis. Diagnostic accuracy assessing fat, capsule and signal intensity at dynamic MRI. J Hepatol. 2012;56:1317-23.
11. Marrero JA, Kulik LM, Sirlin CB, Zhu AX, Finn RS, Abecassis MM, et al. Diagnosis, staging, and management of hepatocellular carcinoma: 2018 Practice Guidance by the American Association for the Study of Liver Diseases. Hepatology. 2018;68:723-50.
12. Roberts LR, Sirlin CB, Zaiem F, Almasri J, Prokop LJ, Heimbach JK, et al. Imaging for the diagnosis of hepatocellular carcinoma: a systematic review and meta-analysis. Hepatology. 2018;67:401-21.
13. Cerny M, Bergeron C, Billiard JS, Murphy-Lavallée J, Olivié D, Bérubé J, et al. LI-RADS for MR imaging diagnosis of hepatocellular carcinoma: performance of major and ancillary features. Radiology. 2018;288:118-28.
14. Joo I, Lee JM, Lee DH, Ahn SJ, Lee ES, Han JK. Liver imaging reporting and data system v2014 categorization of hepatocellular carcinoma on gadoxetic acid-enhanced MRI: comparison with multiphasic multidetector computed tomography. J Magn Reson Imaging. 2017;45:731-40.
15. Choi SH, Byun JH, Kim SY, Lee SJ, Won HJ, Shin YM, et al. Liver Imaging Reporting and Data System v2014 with gadoxetate disodium-enhanced magnetic resonance imaging: validation of LI-RADS category 4 and 5 criteria. Invest Radiol. 2016;51:483-90.
16. Fowler KJ, Tang A, Santillan C, Bhargavan-Chatfield M, Heiken J, Jha RC, et al. Interreader reliability of LI-RADS version 2014 algorithm and imaging features for diagnosis of hepatocellular carcinoma: a large international multireader study. Radiology. 2018;286:173-85.
17. De Gaetano AM, Catalano M, Pompili M, Marini MG, Rodríguez Carnero P, Gullí C, et al. Critical analysis of major and ancillary features of LI-RADS v2018 in the differentiation of small (≤2 cm) hepatocellular carcinoma from dysplastic nodules with gadobenate dimeglumine-enhanced magnetic resonance imaging. Eur Rev Med Pharmacol Sci. 2019;23:7786-801.
18. Di Martino M, Anzidei M, Zaccagna F, Saba L, Bosco S, Rossi M, et al. Qualitative analysis of small (≤2 cm) regenerative nodules, dysplastic nodules and well-differentiated HCCs with gadoxetic acid MRI. BMC Med Imaging. 2016;16:62.

19. Hecht EM, Holland AE, Israel GM, Hahn WY, Kim DC, West AB, et al. Hepatocellular carcinoma in the cirrhotic liver: gadolinium-enhanced 3D T1-weighted MR imaging as a stand-alone sequence for diagnosis. Radiology. 2006;239:438-47.
20. Joo I, Lee JM, Lee DH, Jeon JH, Han JK, Choi BI. Noninvasive diagnosis of hepatocellular carcinoma on gadoxetic acid-enhanced MRI: can hypointensity on the hepatobiliary phase be used as an alternative to washout? Eur Radiol. 2015;25:2859-68.
21. Vernuccio F, Cannella R, Meyer M, Choudhoury KR, Gonzáles F, Schwartz FR, et al. LI-RADS: diagnostic performance of hepatobiliary phase hypointensity and major imaging features of LR-3 and LR-4 lesions measuring 10-19 mm with arterial phase hyperenhancement. AJR Am J Roentgenol. 2019;213:W57-65.
22. Kwon HJ, Byun JH, Kim JY, Hong GS, Won HJ, Shin YM, et al. Differentiation of small (≤2 cm) hepatocellular carcinomas from small benign nodules in cirrhotic liver on gadoxetic acid-enhanced and diffusion-weighted magnetic resonance images. Abdom Imaging. 2015;40:64-75.
23. Granata V, Fusco R, Avallone A, Filice F, Tatangelo F, Piccirillo M, et al. Critical analysis of the major and ancillary imaging features of LI-RADS on 127 proven HCCs evaluated with functional and morphological MRI: lights and shadows. Oncotarget. 2017;8:51224-37.
24. Lee MH, Kim SH, Park MJ, Park CK, Rhim H. Gadoxetic acid-enhanced hepatobiliary phase MRI and high-b-value diffusion-weighted imaging to distinguish well-differentiated hepatocellular carcinomas from benign nodules in patients with chronic liver disease. AJR Am J Roentgenol. 2011;197:W868-75.
25. Piana G, Trinquart L, Meskine N, Barrau V, Beers BV, Vilgrain V. New MR imaging criteria with a diffusion-weighted sequence for the diagnosis of hepatocellular carcinoma in chronic liver diseases. J Hepatol. 2011;55:126-32.
26. Shankar S, Kalra N, Bhatia A, Srinivasan R, Singh P, Dhiman RK, et al. Role of diffusion weighted imaging (DWI) for hepatocellular carcinoma (HCC) detection and its grading on 3T MRI: a prospective study. J Clin Exp Hepatol. 2016;6:303-10.
27. Granata V, Fusco R, Catalano O, Guarino B, Granata F, Tatangelo F, et al. Intravoxel incoherent motion (IVIM) in diffusion-weighted imaging (DWI) for hepatocellular carcinoma: correlation with histologic grade. Oncotarget. 2016;7:79357-64.
28. Nakanishi M, Chuma M, Hige S, Omatsu T, Yokoo H, Nakanishi K, et al. Relationship between diffusion-weighted magnetic resonance imaging and histological tumor grading of hepatocellular carcinoma. Ann Surg Oncol. 2012;19:1302-9.
29. Tang A, Bashir MR, Corwin MT, Cruite I, Dietrich CF, Do RK, et al. Evidence supporting LI-RADS major features for CT- and MR imaging-based diagnosis of Hepatocellular carcinoma: a systematic review. Radiology. 2018;286:29-48.